PNAS

Supporting Information for

Responsiveness to interleukin-15 therapy is shared between tissue-resident and circulating memory CD8$^+$ T cell subsets

Nicholas N. Jarjour[1,2], Kelsey M. Wanhainen[1,2], Changwei Peng[1,2], Noah V. Gavil[1,3], Nicholas J. Maurice[1,2], Henrique Borges Da Silva[1,2], Ryan J. Martinez[1,2], Talia S. Dalzell[1,2], Matthew A. Huggins[1,2], David Masopust[1,3], Sara E. Hamilton[1,2], Stephen C. Jameson[1,2]

Stephen C. Jameson
Email: james024@umn.edu

This PDF file includes:

Figures S1 to S7

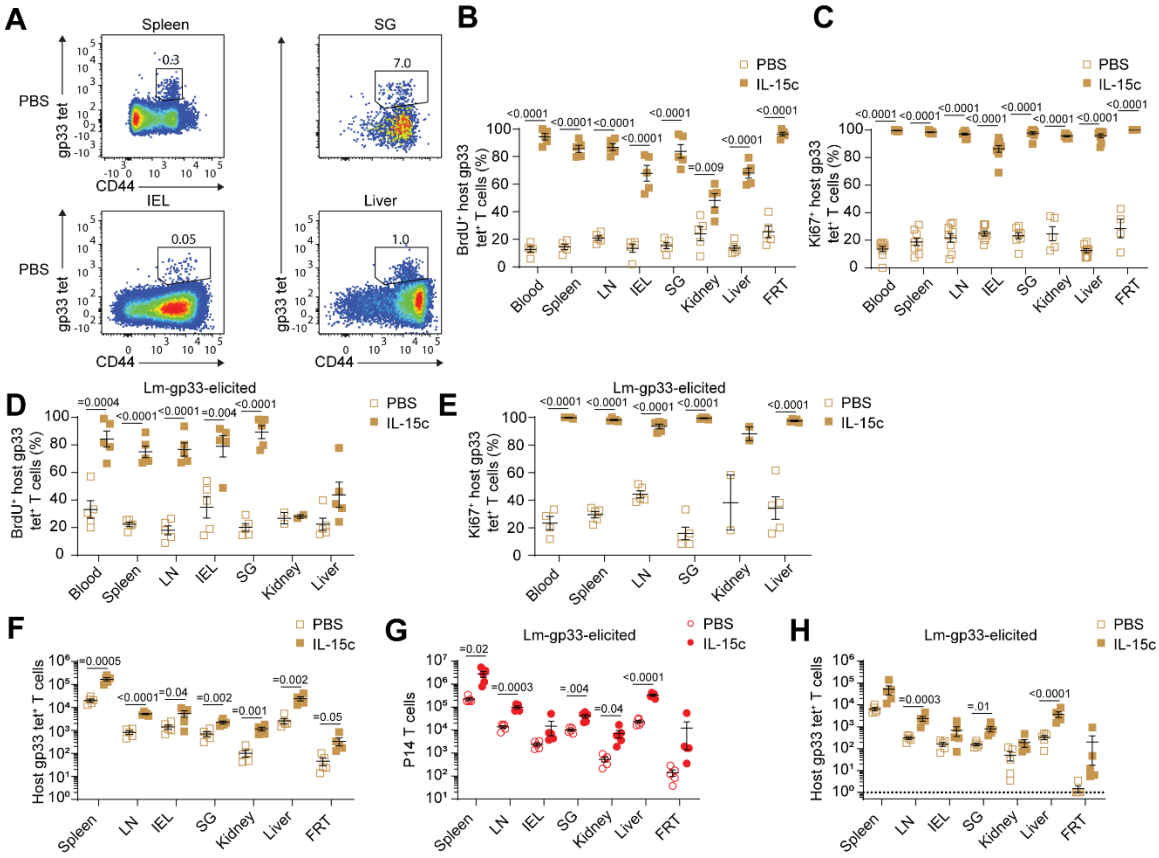

Fig. S1. IL-15c stimulate proliferation and expansion of antigen-specific memory CD8⁺ T cells elicited by viral or bacterial challenge. (A-C) LCMV-elicited P14 memory mice were generated as in Figure 1. **(A)** Flow cytometry for host gp33/D^b tet⁺ CD8⁺ T cells in the spleen, IEL, SG, and liver from PBS-treated mice. **(B,C)** Quantitation of the percentage of (B) BrdU⁺ and (C) Ki67⁺ host gp33/D^b tet⁺ CD8⁺ T cells in the blood, spleen, LN, IEL, SG, kidney, liver, and FRT from PBS- and IL-15c-treated mice, gated as in (A). **(D,E)** Lm-gp33-elicited P14 memory mice were generated as in Figure 2. Quantitation of the percentage of (D) BrdU⁺ and (E) Ki67⁺ host gp33/D^b tet⁺ CD8⁺ T cells in the blood, spleen, LN, IEL, SG, kidney, and liver from PBS- and IL-15c-treated mice. **(F)** LCMV-elicited P14 memory mice were generated as in Figure 1. Quantitation of host gp33/D^b tet⁺ CD8⁺ T cells in the spleen, LN, IEL, SG, kidney, liver, and FRT from PBS- and IL-15c-treated mice. **(G,H)** Lm-gp33-elicited P14 memory mice were generated as in Figure 2. Quantitation of (G) donor P14 and (H) host gp33/D^b tet⁺ CD8⁺ T cells in the spleen, LN, IEL, SG, kidney, liver, and FRT from PBS- and IL-15c-treated mice. (A) Data are representative of 7 experiments with 13-15 mice per group. (B-H) Data are pooled from 2-4 experiments with 4-9 mice per group, except for (D,E) Kidney (2 per group). Unpaired two-sided Student's t tests.

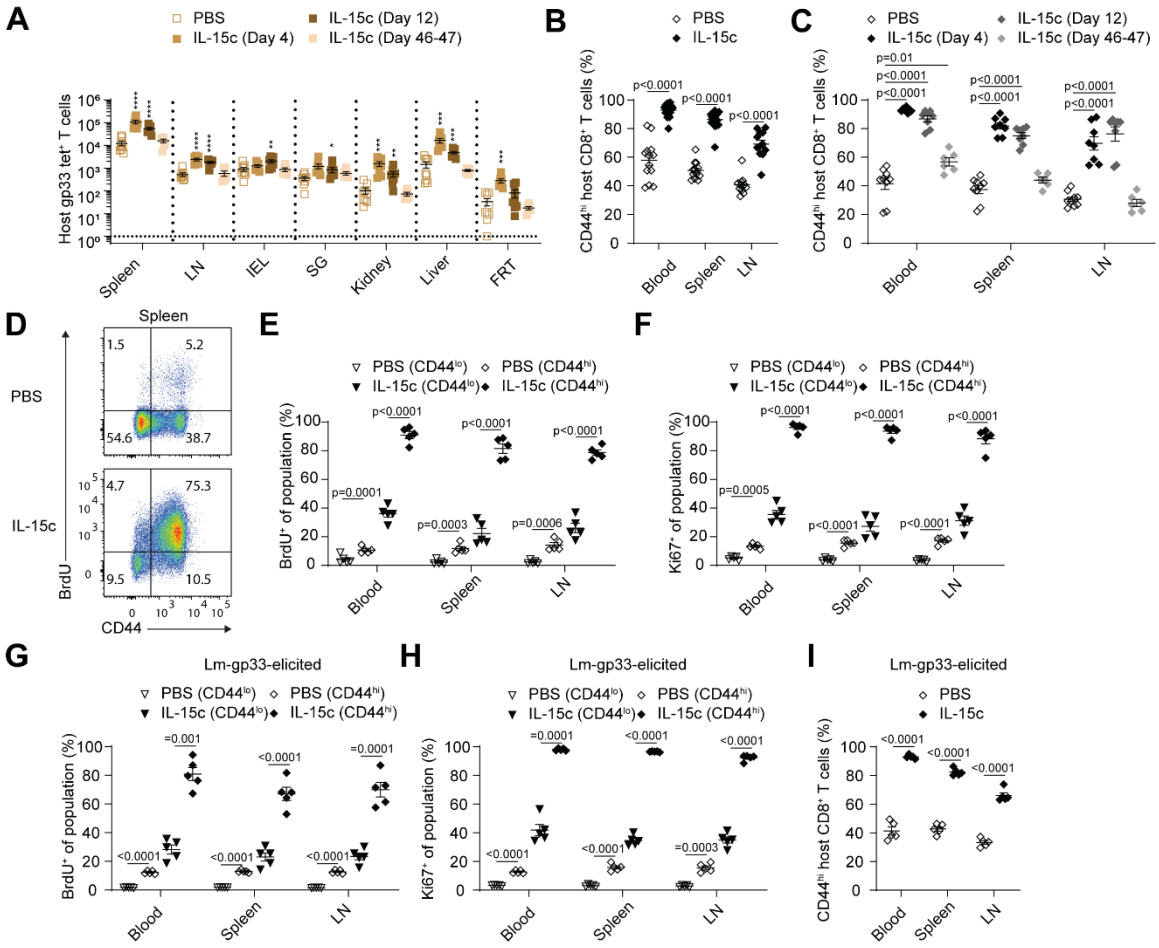

Fig. S2. IL-15c stimulate proliferation and expansion of host antigen-specific memory and memory phenotype CD8⁺ T cells. (A-F) LCMV-elicited P14 memory mice were generated as in Figure 1. (A) P14 memory mice treated as in Fig. 3 were quantitated for host gp33/D^b tetramer-specific $CD8^+$ T cells from the spleen, LN, IEL, SG, kidney, liver, and FRT from PBS- and IL-15c-treated mice on Day 4, Day 12, and Day 46-47 post start of treatment. Dashed line in (A) represents the limit of detection. (B) Quantitation of the percentage of $CD44^{hi}$ host $CD8^+$ T cells in the blood, spleen, and LN from PBS- and IL-15c-treated mice. (C) Quantitation of the percentage of $CD44^{hi}$ host $CD8^+$ T cells in the blood, spleen, and LN from PBS- and IL-15c-treated mice on Day 4, Day 12, and Day 46-47 post start of treatment. (D) Flow cytometry for BrdU incorporation of $CD44^{hi}$ and $CD44^{lo}$ host $CD8^+$ T cells in the spleen from PBS- and IL-15c-treated mice. (E,F) Quantitation of the percentage of (E) $BrdU^+$ and (F) $Ki67^+$ $CD44^{hi}$ (of $CD44^{hi}$ host $CD8^+$ T cells) and $CD44^{lo}$ (of $CD44^{lo}$ host $CD8^+$ T cells) host $CD8^+$ T cells in the blood, spleen, and LN from PBS- and IL-15c-treated mice. **(G-I)** Lm-gp33-elicited P14 memory mice were generated as in Figure 2. (G,H) Quantitation of the percentage of (G) $BrdU^+$ and (H) $Ki67^+$ $CD44^{hi}$ (of $CD44^{hi}$ host $CD8^+$ T cells) and $CD44^{lo}$ (of $CD44^{lo}$ host $CD8^+$ T cells) host $CD8^+$ T cells in the blood, spleen, and LN from PBS- and IL-15c-treated mice. (I) Quantitation of the percentage of $CD44^{hi}$ host $CD8^+$ T cells in the blood, spleen, and LN from PBS- and IL-15c-treated mice. * $p<0.05$; ** $p<0.01$; *** $p<0.001$; **** $p<0.0001$. (A,C) Data are pooled from 2-4 experiments with 6-9 mice per group. (B) Data are pooled from 5-6 experiments with 12-18 mice per group. (D-I) Data are representative of/pooled from 2 experiments with 5 mice per group. (A-C,I) Unpaired and (E-H) paired two-sided Student's t tests.

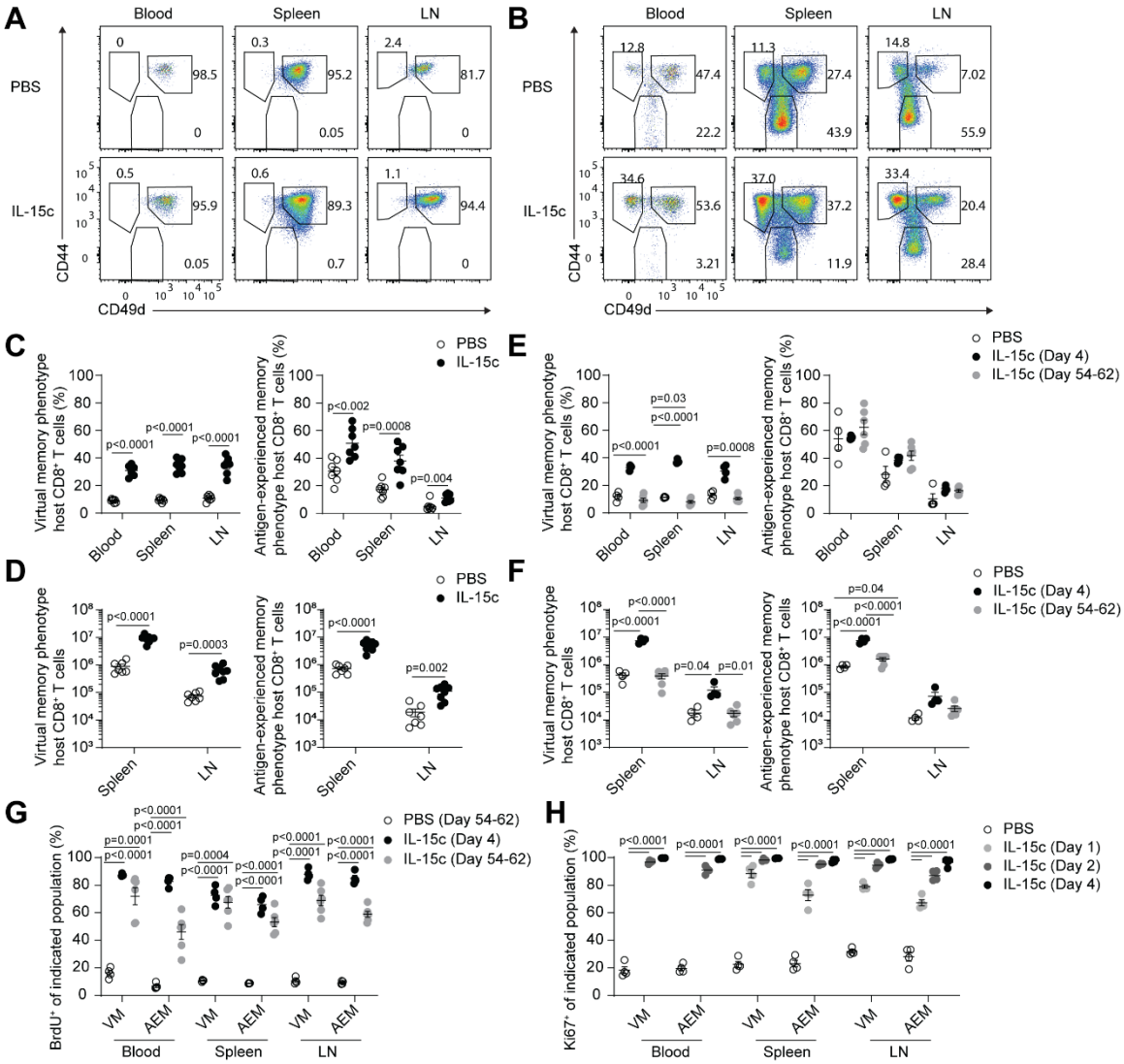

Fig. S3. IL-15c stimulate proliferation and expansion of VM and AEM phenotype host CD8⁺ T cells. LCMV-elicited P14 memory mice were generated as in Figure 1. **(A,B)** Flow cytometry for CD49d and CD44 expression of (A) donor memory P14 T cells and (B) host CD8⁺ T cells in the spleen from PBS- and IL-15c-treated mice. **(C,D)** Quantitation of the (C) percentage (of all host CD8⁺ T cells) and (D) number of VM and AEM cells in the blood (percentage only), spleen, and LN from PBS-treated and IL-15c mice, gated as in (B). **(E,F)** Quantitation of the (E) percentage (of all host CD8⁺ T cells) and (F) number of VM and AEM cells in the blood (percentage only), spleen, and LN from PBS-treated and IL-15c-treated mice on Day 4 and Day 54-62 post start of treatment, gated as in (B). **(G)** Quantitation of the percentage of BrdU⁺ host VM and AEM cells in the blood, spleen, and LN from PBS- and IL-15c-treated mice on Day 4 and Day 54-62 post start of treatment, with BrdU labelling for the PBS- and IL-15c-treated pulse-chase groups from Day 0-6 only. **(H)** Quantitation of the percentage of Ki67⁺ host VM and AEM cells in the blood, spleen, and LN from PBS- and IL-15c-treated mice on Days 1, 2, and 4 post start of treatment. Data are representative of/pooled from 2-3 experiments with 4-7 mice per group. Unpaired two-sided Student's t tests.

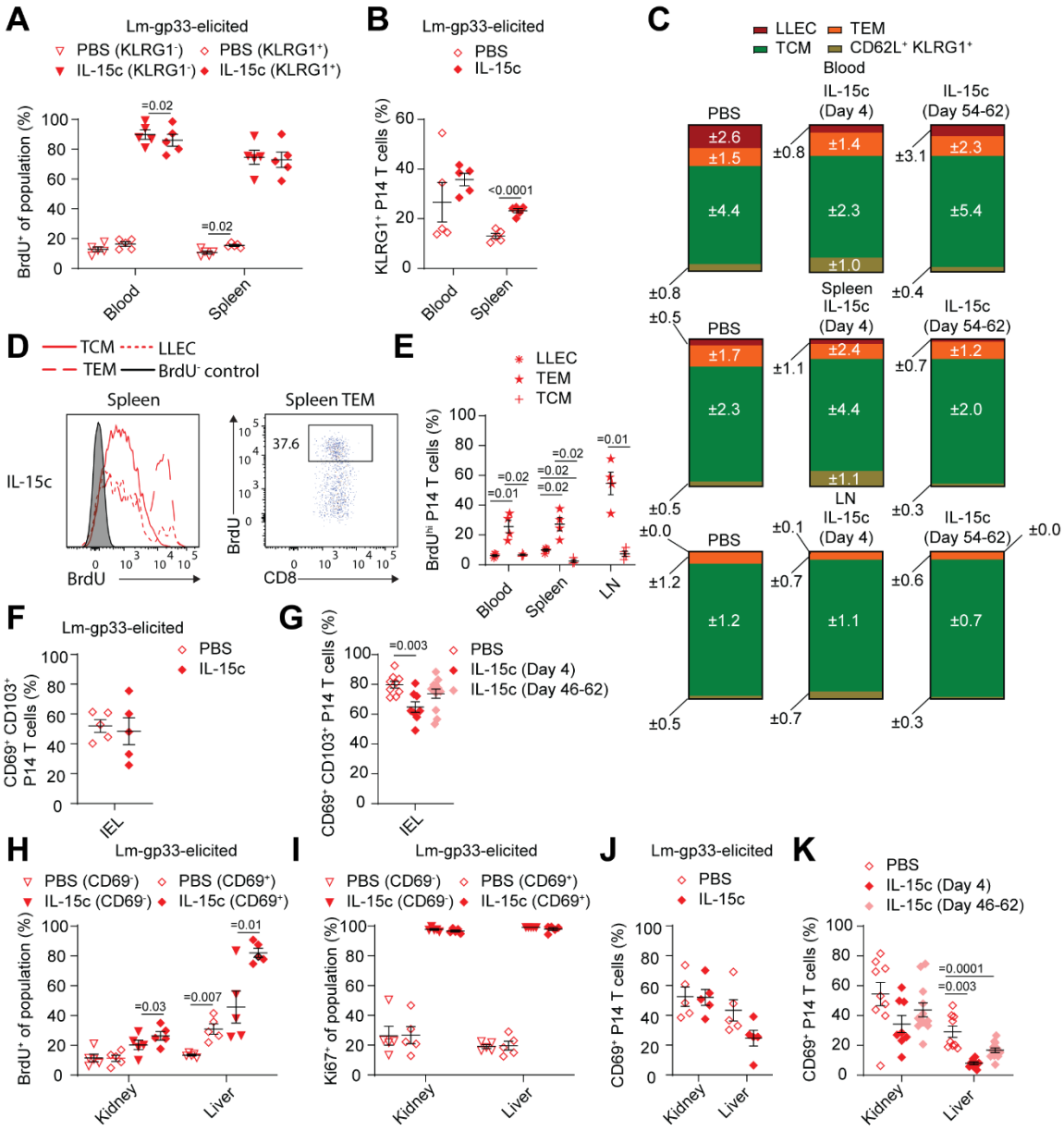

Fig. S4. IL-15c stimulate proliferation and expansion of antigen-specific resident and recirculating memory subsets. (A,B) Lm-gp33-elicited P14 memory mice were generated as in Figure 2. (A) Quantitation of the percentage of BrdU$^+$ KLRG1$^+$ (of KLRG1$^+$ P14 T cells) and KLRG1$^-$ (of KLRG1$^-$ P14 T cells) donor P14 T cells in the blood and spleen. (B) Quantitation of the percentage of KLRG1$^+$ donor P14 T cells (of all donor P14 T cells) in the blood and spleen from PBS- and IL-15c-treated mice. **(C-E)** LCMV-elicited P14 memory mice were generated as in Figure 1. (C) Quantitation of the percentages of P14 circulating memory subsets in the blood, spleen, and LN from PBS- and IL-15c-treated mice on Day 4 and Day 54-62 post start of treatment (Days 110-120 post-LCMV). Values represent standard error of the mean. (D) Flow cytometry for BrdU incorporation expressed as a (Left) histogram overlay for LLEC, T_{EM}, and T_{CM} P14 T cells (versus a BrdU-negative control sample) and (Right) pseudocolor plot gated for BrdU^{hi} T_{EM} P14 T cells in the spleen of an IL-15c-treated mouse. (E) Quantitation of the percentage of BrdU^{hi} LLEC, T_{EM}, and T_{CM} P14 T cells in the blood, spleen, and LN (T_{EM} and T_{CM} only) from IL-15c-treated mice, gated as in (D). **(F)** Quantitation of the percentage of CD69$^+$ CD103$^+$ donor IEL P14 T cells (of all donor P14 T cells) from PBS- and IL-15c-treated Lm-gp33-elicited P14 memory mice. **(G)** Quantitation of the percentage of CD69$^+$ CD103$^+$ donor IEL P14 T cells (of all donor P14 T cells) from PBS- and IL-

15c-treated LCMV-elicited P14 memory mice on Day 4 and Day 46-62 post start of treatment. **(H,I)** Quantitation of the percentage of (H) $BrdU^+$ and (I) $Ki67^+$ $CD69^+$ (of $CD69^+$ P14 T cells) and $CD69^-$ (of $CD69^-$ of P14 T cells) donor P14 T cells in the kidney and liver from PBS- and IL-15c-treated Lm-gp33-elicited P14 memory mice. **(J)** Quantitation of the percentage of $CD69^+$ donor P14 T cells (of all donor P14 T cells) in the kidney and liver from PBS- and IL-15c-treated Lm-gp33-elicited P14 memory mice. **(K)** Quantitation of the percentage of $CD69^+$ donor P14 T cells (of all donor P14 T cells) in the kidney and liver from PBS- and IL-15c-treated LCMV-elicited P14 memory mice on Day 4 and Day 46-62 post start of treatment. Data are pooled from 2-4 experiments with 4-12 mice per group. (B,F,G,J,K) Unpaired and (A,E,H,I) paired two-sided Student's t tests.

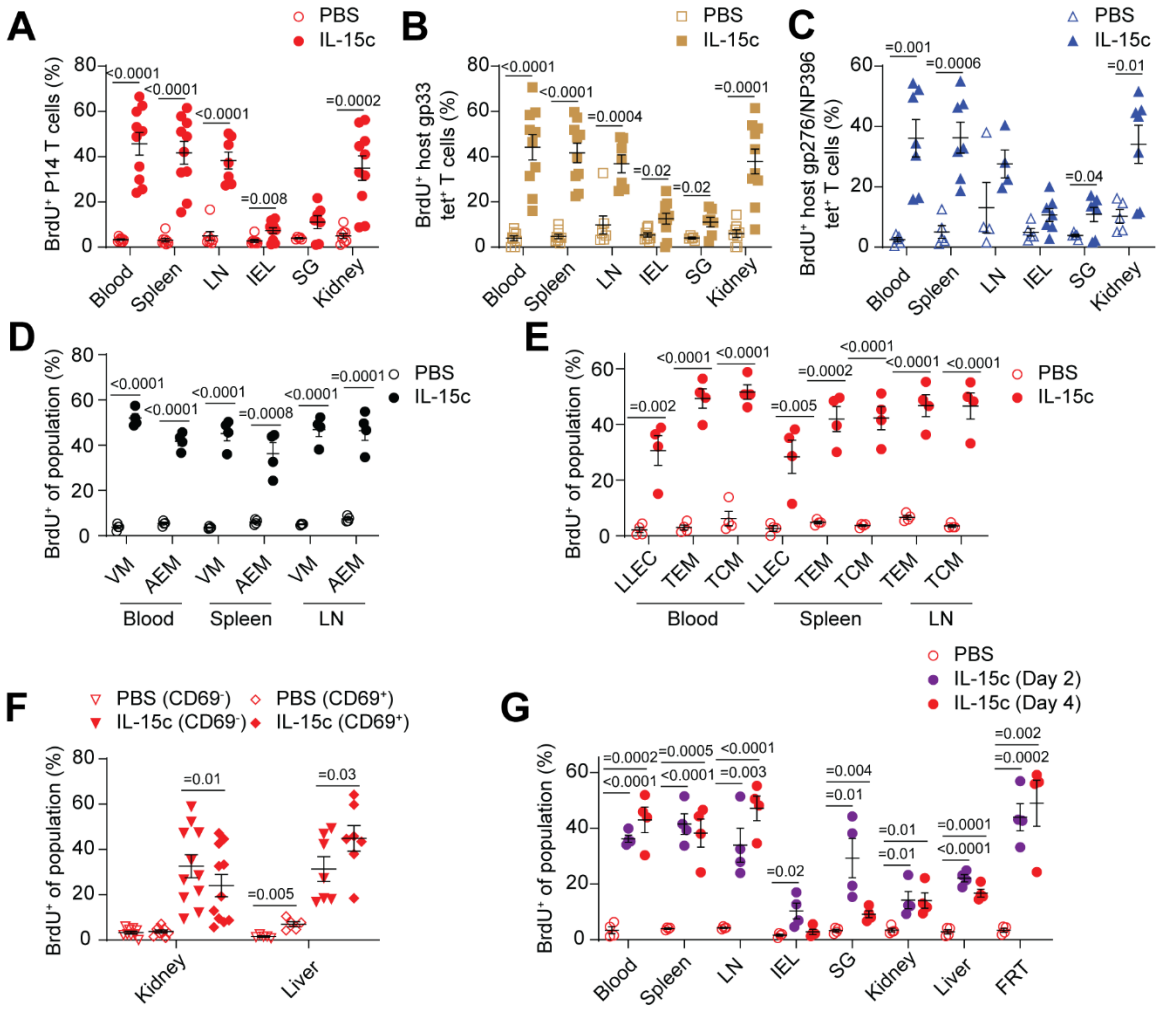

Fig. S5. Short-term BrdU labelling after IL-15c is consistent with local proliferation within tissue sites. LCMV-elicited P14 memory mice were generated and treated with PBS and IL-15c as in Figure 1. Instead of longitudinal labelling, 24 hours before sacrifice, BrdU was given i.p. **(A-C)** Quantitation of the percentage of BrdU⁺ (A) donor P14, (B) host gp33/D^b tet⁺, and (C) host gp276/NP396/D^b tet⁺ CD8⁺ T cells in the blood, spleen, LN, IEL, SG, and kidney from PBS- and IL-15c-treated mice. **(D)** Quantitation of the percentage of BrdU⁺ VM and AEM host CD8⁺ T cells in the blood, spleen, and LN from PBS- and IL-15c-treated mice. **(E)** Quantitation of the percentage of BrdU⁺ LLEC, T_{EM}, and T_{CM} in the blood, spleen, and LN (T_{EM} and T_{CM} only) from PBS- and IL-15c-treated mice. **(F)** Quantitation of the percentage of BrdU⁺ CD69⁺ (of CD69⁺ P14 T cells) and CD69⁻ (of CD69⁻ of P14 T cells) donor P14 T cells in the kidney and liver from PBS- and IL-15c-treated mice. **(G)** Quantitation of the percentage of BrdU⁺ donor P14 T cells in the blood, spleen, LN, IEL, SG, kidney, liver, and FRT from PBS- and IL-15c-treated mice on Day 2 and Day 4 post start of treatment. BrdU was given i.p. 24 hours before sacrifice (Day 2 cohort, BrdU given on Day 1. Day 4 cohort, BrdU given on Day 3). Data are pooled from 2-5 experiments with 4-11 mice per group. (A-E,G) Unpaired and (F) paired two-sided Student's t tests.

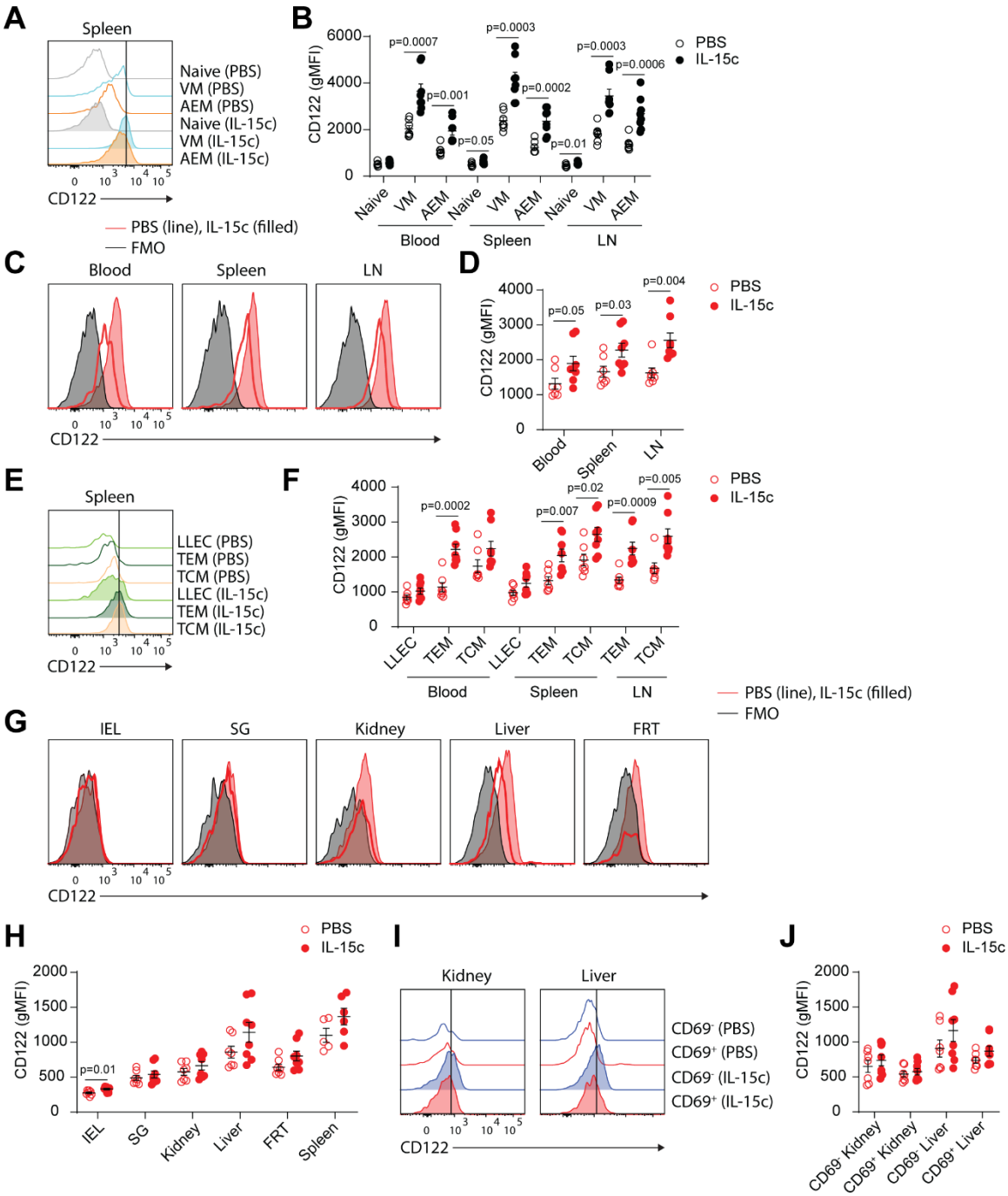

Fig. S6. CD122 expression differs across memory CD8⁺ T cell subsets. LCMV-elicited P14 memory mice were generated and treated with PBS and IL-15c as in Figure 1. **(A)** Flow cytometry for CD122 expression on naïve, VM, and AEM host CD8⁺ T cells in the spleen from PBS- and IL-15c-treated mice. **(B)** Quantitation of CD122 geometric mean fluorescence intensity (gMFI) on naïve, VM, and AEM host CD8⁺ T cells in the blood, spleen, and LN from PBS- and IL-15c-treated mice. **(C)** Flow cytometry for CD122 expression on donor P14 T cells in the blood, spleen, and LN from PBS- and IL-15c-treated mice, compared to a fluorescence minus one (FMO) control for CD122 staining. **(D)** Quantitation of CD122 gMFI on donor P14 T cells in the blood, spleen, and LN from PBS- and IL-15c-treated mice. **(E)** Flow cytometry for CD122 expression on LLEC, T_{EM}, and T_{CM} donor P14 T cells in the spleen from PBS- and IL-15c-treated mice. **(F)** Quantitation of CD122 gMFI on LLEC, T_{EM}, and T_{CM} donor P14 T cells in the blood, spleen, and LN (T_{EM} and T_{CM} only)

from PBS- and IL-15c-treated mice. **(G)** Flow cytometry for CD122 expression on donor P14 T cells in the IEL, SG, kidney, liver, and FRT from PBS- and IL-15c-treated mice, compared to a fluorescence minus one (FMO) control for CD122 staining. **(H)** Quantitation of CD122 gMFI on donor P14 T cells in the IEL, SG, kidney, liver, and FRT from PBS- and IL-15c-treated mice. **(I)** Flow cytometry for CD122 expression on $CD69^+$ and $CD69^-$ donor P14 T cells in the kidney and liver from PBS- and IL-15c-treated mice. **(J)** Quantitation of CD122 gMFI on $CD69^+$ and $CD69^-$ donor P14 T cells in the kidney and liver from PBS- and IL-15c-treated mice. (A,B,D-F,H-J) Data are representative of/pooled from 3 experiments with 7-8 mice per group. (C,G) Data are representative of 1 experiment with 3-4 mice per group. Unpaired two-sided Student's t tests.

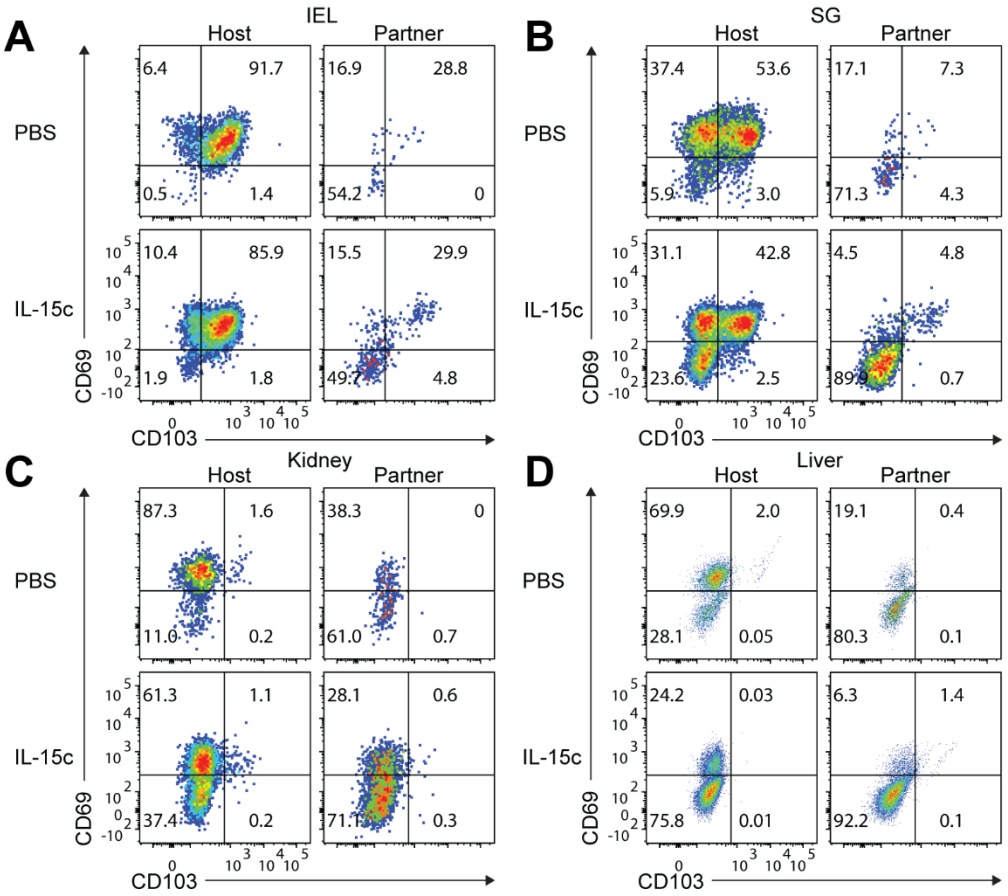

Fig. S7. Phenotype of NLT donor- and partner-derived P14 T cells after IL-15c treatment. (A-D) Flow cytometry for CD69 and CD103 expression on host and partner P14 T cells in the (A) IEL, (B) SG, (C) kidney, and (D) liver from PBS- and IL-15c-treated parabiosed mice as in Fig. 5. Representative of 3 experiments with 3-4 parabiosed pairs per group.